# APPLICATION OF NEGATIVE SCARF TO INLET DESIGN FOR ACOUSTIC REDUCTION, AERODYNAMIC ASSESSMENT AT SUBSONIC & TRANSONIC SPEEDS

**Dr. R. K. Nangia & Dr. M. E. Palmer**
**Nangia Aero Research Associates,**
**Maggs House, 78-Queens Road,**
**BRISTOL, BS8 1QX, UK.**
**Tel: +44 (0)117-987 3995 Fax: +44 (0)117-987 3995**

## ABSTRACT

*Aircraft engines must meet current and future FAR regulations and noise "footprints" criteria. A way of reducing noise is to use negatively scarfed inlets. The extended lower lip acts as an acoustic "barrier". We need to understand the aerodynamic implications of inlet scarfing at low and transonic speeds.*

*The subsonic aerodynamic performance (incidence, side-slip and ground effects) of a conventional (+6° scarf) inlet has been assessed. A range of negative scarf angles was applied to the geometry and the subsonic performance of the resulting inlets assessed. A staged, iterative design process was carried out on a -20° scarfed inlet from this series. This led to modified lip geometry that gave attached flow capability equivalent to the datum "conventional" inlet. An additional advantage for negative scarf was the weakening of the ground vortex at "zero forward speed". This is important for "large" intakes with high by-pass ratios, set closer to the ground.*

*The transonic performance of the conventional (+6° scarf) and negatively scarfed inlet (-20°) was assessed. A limited design study was carried out on the -20° inlet to understand the effects of lip shaping at high speed (Mach 0.8). An encouraging equivalence has been achieved between the datum and scarfed inlet and further detailed work (internal surfaces) leading to experiments has been recommended. Work is needed on scarf angle choice.*



## 1. INTRODUCTION & BACKGROUND

The environmental demands for quieter, more efficient, civil aircraft, **Fig.1**, are major design constraints (Ref.1). The trend is towards higher by-pass ratios implying large engines. Power demands are increasing (bigger aircraft with fewer engines) and this encourages large engines. The increase in size/power produces more fan noise. The engines will be closer to the ground during take-off (ramp to lift-off) and landing (touch-down to ramp) resulting in stronger ground vortices and increased possibility of foreign object damage. Civil engines must meet current / future noise standards in the flight envelope, **Fig.2**.

For military aircraft, efficiency and noise reduction are not major design criteria, although noise reduction in terms of stealth performance would be welcome as would extended range or duration.

Several techniques for noise reduction are being investigated in Europe and the USA. These include engine components, active noise control, noise absorbent coatings and inlet geometry. The latter has led to a study of negatively scarfed inlets and design/airframe interactions.

Intake noise "radiation" and various options for its reduction are sketched in **Fig.3**. A conventional (+6° scarf), wing mounted, isolated inlet, is shown in **Fig.3(a)**. Noise, generated by the compressor blades, escapes, either directly or after reflection from the internal surfaces. With zero scarf, noise escapes equally in all directions radially. The extended upper lip of the +6° scarfed inlet reflects a larger proportion of the noise towards the ground. This can be reduced by applying noise absorbent coatings or baffles to the inner surfaces. Negative scarf may be applied in several ways, **Fig.3(b)**. Pivoting the highlight about the top LE extends the lower lip, increasing overall weight. Pivoting about the bottom LE reduces the top lip length but adversely affects aerodynamic properties.

Pivoting about the horizontal, transverse, datum is a compromise which leaves the overall weight almost unchanged. The extended lower lip reflects more noise upwards, shielding the ground from much of the direct and reflected noise. The aerodynamic properties of the top lip may need improvement. Rotating a scarfed inlet about its longitudinal axis re-directs noise away from the aircraft cabin, **Fig.3(c)**. Modifications to the nacelle / pylon / wing design are noted in **Fig.3**.

An additional advantage of negative scarfed inlets is a reduction in ground vortex strength indicated by reduced surface velocities on the lower lip.

### Previous & Related Work on Scarfed Inlets

Experimental work (low and high speed) on inlet scarfing to reduce noise output has been reported in Refs.2-3. Increased $\alpha$ capability for scarfed inlets in terms of engine face pressure distortions, at power on, take-off conditions was indicated. At windmill conditions there was a reduced $\alpha$ capability. The $\alpha$ capability was based purely on assessments of $\alpha$ at which engine face distortions reached a pre-determined "acceptable" limit. The distortions may be caused by a variety of factors including internal lip flow separation, shock-induced throat flow separation or flow separation from the diffuser wall. It was also noted in Refs.2 & 3 that scarfed inlets have limited attached flow ranges under cross-wind conditions. The internal upper lip needs to cater for cross-wind conditions.

Ref.4 looked at the performance of a similar type of inlet at low subsonic and "zero forward-speed" with & without cross-wind. Performance was assessed in terms of attached flow ranges ($\alpha$ and $\beta$ capability) using onset of lip flow separation predictions (Ref.5). In this way a greater understanding of the factors contributing to engine face distortions may be gained. The effects of highlight scarf angle were assessed. An in-house developed inlet design method was applied to the scarfed inlets, modifying various sections around the highlight to bestow optimised subsonic attached flow capabilities (Ref.6). The "zero forward-speed" aspect (Ref.7) was also covered.

### This Paper

We study design implications (aerodynamic and structural) of applying negative scarf. Attached flow ranges for a "conventional" inlet with modest, positive scarf, are established and the effects of negative scarf are assessed. A negative scarfed inlet is then redesigned so as to regain the subsonic performance of the "conventional" inlet. The transonic performance of the "designed" inlet is then assessed and modified to improve its performance.

## 2. DESIGN PROCESS FOR INLET PROFILE

The design process is iterative, **Fig.4**. Subsonic, transonic, supersonic, incidence and side-slip factors are considered, with varying degrees of importance, at each loop of the design process. Most important are the low speed, $\alpha$, handling aspects (take-off and landing). The design at this stage must consider environmental constraints. Side-slip effects at low speed are next important and certification requirements must be met. At high speed (cruise), economic factors dominate the design process and low drag and high inlet efficiency become the driving factors. The full design scheme would

need to consider low and high speed, $\alpha$ and $\beta$, ground effects and installation effects.

Inlet performance (attached flow range) is assessed, at discrete points around the highlight. The performance may be improved by modifying the local streamwise profile to extend or shift the attached flow ranges. In very general terms, the application of camber, locally, will shift the attached flow band without altering its range. Changes to local thickness will extend or reduce the attached flow range about a nominal mean.

An in-house developed code, Ref.5, was used for the low-speed / subsonic calculations and an unstructured mesh Euler code, Ref.8, was used for the high speed work.

## 3. LOW SPEED CHARACTERISTICS

The effects of inlet scarf angle on the aerodynamic characteristics were studied at M = 0.25 over $\alpha$ and $\beta$ ranges. Attached flow ranges were obtained at a Reynolds number (Re) based on inlet highlight diameter ($D_h$)

Effect of Incidence & Scarf angle at M = 0.25.

The four scarf angle cases (+6°, 0°, -10° & -20°, inlets A, B, C & D respectively) were assessed at $\alpha$ = 0°, 10° and 20° to gain an understanding of the trends associated with scarf and incidence.

Peak LE velocities ($V_{Tmax}$), around the inlet highlight, are shown in **Fig.5** for Inlets-A and -D (scarf +6° & -20°) at $\alpha$ = 0°, M = 0.25. $V_{Tmax}$ variation at $\alpha$ = 20°, M = 0.25 is shown in **Fig.6**.

Negative scarfing has significantly increased the LE velocities at the top of the inlet, increasing the possibility of lip flow separation. The lower lip has reduced peak velocities. At incidence ($\alpha$ = 20°), the trends due to scarfing are similar.

The attached flow ranges, for Inlets-A and -D, at M = 0.25, Re = $3.0 \times 10^6$, $\alpha$ = 0° are shown in **Fig.7**. Inlet-A (+6° scarf) has fully attached flow over a large MFR range, from below windmilling to above full power ($M_{EF}$ = 0.625). Inlet-D (-20° scarf) has a reduced MFR operating range. Internal flow separation is induced at the top lip when $M_{EF}$ = 0.475. Other regions around the highlight of Inlet-D have extended MFR operating ranges. Re-design of the profile (camber, LE radius and thickness) of the top lip and adjacent areas would regain much, if not all, of the Datum Inlet-A attached flow MFR range.

At incidence ($\alpha$ = 20°), Inlet-A experiences early internal flow separation (increasing MFR) at the bottom lip, **Fig.8**. As MFR reduces, external flow separation occurs at the top lip at MFR just above windmilling. Scarfing the highlight by -20° does not have a significant effect on the overall inlet performance. External flow separation onset at the top of the inlet occurs earlier as MFR reduces. Over the bottom half of the inlet, internal flow separation occurs slightly earlier.

### Effect of Side-Slip & Scarf angle at M = 0.25.

To understand the trends associated with side-slip and scarf, the four inlets (A, B, C & D) were assessed at $\alpha$ = 0°, $\beta$ = 0°, 5° and 10° (positive $\beta$, nose to left). At M = 0.25, $\beta$ = 10° implies a cross-wind of 15m/s (29kts).

Details of $V_{Tmax}$ variations around the highlight are given in Ref.9 for Inlets-A, -B, -C and -D at $\alpha$ = 0°, $\beta$ = 10°, M = 0.25. Corresponding attached flow ranges are shown in **Fig.9**. At low $V_N$ (windmilling), high velocities on the leeward side of Inlet-A indicate the possibility of external separation. At high $V_N$, high velocities on the windward side of Inlet-A give rise to internal flow separations. In comparative terms, the top and bottom regions of Inlet-A are well behaved, with a correspondingly lower possibility of separation, **Fig.9.**

Scarfing the inlet (-20°) has increased the LE velocities at the top of the inlet at both high and low $V_N$. This would suggest early flow separation both internal (high $V_N$) and external (low $V_N$), resulting in a reduced operating range for the top cowl-lip (**Fig.9**). Ref.2 noted that scarfed inlets have limited ranges of attached flow in cross-wind conditions and that the internal upper lip needs to be designed to

accommodate this. The velocities at the bottom of the inlet have not been greatly affected by scarfing. As may be expected, the LE peak velocities and attached flow ranges of the leeward and windward sides of the inlet have not been greatly affected by scarfing.

## 4. "ZERO" SPEED WITH & WITHOUT GROUND

Flow vectors (y-z plane), streamlines (x-z plane) and VTmax variation at "zero forward-speed", are shown in **Fig.10** for Inlets-A and -D (+6°, -20°). The ground effects are also shown. As expected, in free air, more flow from above the z = 0 plane is induced into the negatively scarfed inlet than for Inlet-A. This effect is amplified by ground.

A ground vortex is evident in **Fig.10(b)**. Analysis of the current results has confirmed an earlier conclusion that negative scarf reduces the ground vortex strength. This is an important advantage as engine inlets become larger and lie closer to the ground.

At "zero forward-speed", Inlet-D has slightly increased $V_{Tmax}$ at the top with reduced values at the bottom compared to Inlet-A, **Fig.10(c & d)**. A line indicating the sonic limit for $M_{EF}$ = 0.5 is shown. For Inlet-D, $V_{Tmax}$ over the top half of the inlet is above the sonic limit suggesting onset of internal flow separation.

Increments in VTmax due to ground effect are more beneficial on Inlet-D (-20°) than on Inlet-A (+6°), **Fig.11**. For Inlet-A, $V_{Tmax}$ is reduced by 7.0% at the bottom whereas it increases by 3.5% at the top. For Inlet-D these figures are 8.5% (larger improvement) and only 1.5% respectively. These values will change as we` proceed towards more optimum lip shapes and flow separation onset at "zero forward-speed" is explored in more detail.

## 5. SUBSONIC DESIGN STAGE AND LOW SPEED CHARACTERISTICS

Starting with a conventional, near axi-symmetric inlet with positive scarf (Inlet-A, +6°), negative scarf was applied (0°, -10°, -20°) and the subsonic aerodynamic performance of the resulting inlets assessed. Modifications to the local profiles of the negatively scarfed inlets were applied to restore and improve upon the low-speed, $\alpha$ = 0°, performance of Inlet-A. This was achieved by altering the thickness distribution. For -20° scarf, the resulting Inlet-E, **Fig.12**, has a much thicker top lip and a thinner bottom lip. This re-distribution of thickness on the negatively scarfed inlet is a direct means of regaining the attached flow range of the datum Inlet-A taking into account subsonic considerations only.

The lip attached flow ranges, for Inlets-A and -E, at M = 0.25, Re = $3.0 \times 10^6$, $\alpha$ = 0° are shown in **Fig.13**. The designed, -20° scarfed, Inlet-E has achieved 95% of the attached flow operating range of the datum Inlet-A. The transonic aspects of these two inlets are now assessed.

## 6. TRANSONIC CHARACTERISTICS

During a typical long range flight, the engine face Mach number ($M_{EF}$) varies significantly. For example, at the beginning of cruise, $M_{EF}$ is nearer 0.6. At the end of cruise (lighter aircraft), $M_{EF}$ is near 0.5.

### Calibration Phase & Selection of $M_{EF}$ (Datum) Inlet-A

For free-stream Mach number $M_0$ = 0.8, $\alpha$ = 0°, the effect of varying engine face Mach number ($M_{EF}$) was studied, Ref.10. An increase in LE suction over the bottom lip as $M_{EF}$ reduced was noted. For nominal $M_{EF}$ = 0.4, there were distortions across the engine face ($0.38 < M_{EF} < 0.42$) and the appearance of a shock over the outer lip.

For the remaining work, we have emphasised $M_{EF}$ of 0.5. This is also a more "challenging" case for studying onset of external lip separations or shocks, Ref.10.

### Effect of a on Inlet-A (+6° Scarf) at M = 0.80

For $M_0$ = 0.8 & $M_{EF}$ = 0.5, **Fig.14** shows the effect of incidence ($\alpha$ = 0°, 1°, 2°, & 4°) on Mach number and Cp distributions at three stations, $\Phi$ = 0°, 90° & 180°. This is supported by Mach number contours at $\alpha$ = 0° and 4°,

**Figs.15 & 16**, on the outer and inner surfaces and cuts through the mean symmetry plane. As incidence increases, the lower lip off-loads at the expense of higher loading over the top lip, **Fig.14**. At $\alpha$ = 0ø, the Mach contours, **Fig.15**, indicate a region on the external surface where M approaches 1.45. As incidence is increased to $\alpha$ = 4°, **Fig.16**, the supersonic regions reduce in magnitude (1.32 max) and extent, indicating that this particular inlet was designed for an upwash flow angle of about 5°.

### Inlet-E (-20ø Scarf) at M = 0.80, a = 0°

The lines for this inlet were derived from those of Inlet-A by scarfing from +6° to -20° and modifying the thickness distribution around the highlight to regain the $\alpha$ = 0° subsonic performance of Inlet-A.

For $M_0$ = 0.8 & $M_{EF}$ = 0.5, Mach number contours of **Fig.17** show the presence of a strong local shock over the top lip. This meant that camber changes were required to reduce the local velocities.

## 7. TRANSONIC DESIGN STAGE

### Inlets-F & -G (-20ø Scarf)

The lines for these inlets were derived from Inlet-E by applying inwards camber at the top station ($\Phi$ = 180°) fading to zero at $\Phi$ = 135°. Opposite camber was applied along the remainder of the highlight semi-perimeter (+135° > $\Phi$ > 0°) with maximum opposite camber at $\Phi$ = 60° to ensure that $A_h$ remained unaltered from Inlet-A. For Inlet-F, inwards camber of 0.023d at LE was applied at the top station. Additional inwards camber of 0.023d was applied at the top for Inlet-G. The inlets are symmetrical about the vertical centre-line.

For $M_0$ = 0.8, $M_{EF}$ = 0.5, Mach & Cp distributions for Inlets-E, -F and -G, are shown in **Fig.18**. A notable reduction in peak surface M (from 1.52 to 1.39) for Inlet-F with respect to Inlet-E is noted at $\alpha$ = 0°. The reduction in peak surface M obtained with the second camber increment is not as significant. Also, further high suction areas develop on the external surface of Inlet-G. This emphasises the non-linearity. Note the progressive reduction of lip suctions over the top lip with most of the effect being achieved with lip changes up to Inlet-F.

The geometry of Inlet-F was therefore preferred as being more suitable for further exploratory design changes and comparison with the datum Inlet-A.

## 8. COMPARISONS, DATUM INLET-A & NEGATIVELY SCARFED INLET-F

Mach number and Cp distribution comparisons for Inlets-A and -F at $M_0$ = 0.8, $M_{EF}$ = 0.5 and $\alpha$ = 0° were made in Ref.10. It was noted that LE suctions over the top lip of Inlet-F (-20° scarf) were no worse than those on the bottom lip of the datum Inlet-A (+6°). There is room for improvement of the LE suctions on the bottom lip of Inlet-F which needs to be slightly more rounded. At $\alpha$ = 4°, large suction regions occur at the top of Inlet-F, **Fig.19**, suggesting further design work for $\alpha$ tolerance.

With just a few geometry variations, we have broadly achieved a reasonable equivalence between the datum and negatively scarfed inlets. This is encouraging. Of course, detail improvements are still needed e.g. (internal surfaces). These are under consideration using inverse design techniques (Ref.11). Another design cycle through the subsonic process will be required. The question of how much scarf is needed remains open for further acoustic studies. A case for experimental verification can be made.

## 9. CONCLUDING REMARKS & FURTHER WORK

Negatively scarfed inlets have significant acoustic benefits. A -20° scarfed inlet has been modified, using a single pass through a design process, so as to regain 95% of the subsonic performance of a conventional, +6° scarfed inlet. The "designed" inlet was then further modified to improve its transonic performance. Reasonable equivalence between the conventional and negatively scarfed inlets has been achieved. The encouragement from the

work presented should stimulate further activity e.g.

- Detailed analysis of negatively scarfed inlets in the transonic regimes using a 3-D inverse design process (Ref.9). The question of how much scarf is needed needs to be addressed.
- Additional 3-D tailoring of the negatively scarfed inlet to reduce cabin noise.
- Application of scarf angle will involve integrated design of the nacelle/pylon/wing configuration particularly at transonic conditions.
- Experimental verification at several levels with Reynolds number effects.

Reducing the top lip length has repercussions in terms of structure of nacelle/wing pylon. The thickening of the top lip for aerodynamic reasons would allow more robust pylon/nacelle attachments.

In conclusion, existing methods have shown that negative scarf is another viable design option to consider for intake noise reduction and the scene has been set for experimental verification at several levels.

## ACKNOWLEDGEMENTS

The authors have pleasure in acknowledging helpful technical discussions with several Scientists from Rolls Royce (UK) & GE (USA). The work reported is a part of in-house R & D.

## REFERENCES

[1] PACULL, M., "Community Noise, Current Situation and Future Challenges", CEAS 7th European Propulsion Forum "Aspects of Engine / Airframe Integration", March 1999, Pau, France.

[2] CRUM, T.S., YATES, D.E., ANDREW, T.L. & STOCKMAN, N.O., "Low Speed Test Results of Subsonic, Turbofan Scarf Inlets", AIAA/SAE/ASME/ASEE 29th Joint Propulsion Conference & Exhibit, AIAA 93-2301, June 1993, Monterey, CA.

[3] ANDREW, T.L., YATES, D.E., CRUM, T.S., STOCKMAN, N.O., & LATAPY, M.O., "High Speed Test Results of Subsonic, Turbofan Scarf Inlets", AIAA/SAE/ASME/ASEE 29th Joint Propulsion Conference & Exhibit, AIAA 93-2302, June 1993, Monterey, CA.

[4] NANGIA, R.K. & PALMER, M.E., "Negatively Scarfed Inlets for Acoustic Reduction, Aerodynamic Performance Assessment", AIAA 2000-0354, AIAA 38th Aerospace Sciences Meeting, Reno, Jan. 2000.

[5] NANGIA, R.K., PALMER, M.E. & MARTIN, P.G., "Flow Separation Prediction on Three Dimensional Intakes with Mach & Reynolds Number Effects in Subsonic Flight", RAeS - IMechE Conference "Engine-Airframe Integration", October 1996, Bristol, UK.

[6] NANGIA, R.K., PALMER, M.E. & HODGES, J., "Modelling of 3-D Aircraft Inlets at 'Zero' Speed (& Low Speeds with Cross-Wind) & Flow Separation Prediction", RAeS - IMechE Conference "Verification of Design Methods by Test & Analysis", November 1998, London, UK.

[7] NANGIA, R.K., PALMER, M.E. & HODGES, J., "Addressing the 'Zero Speed' & Low-Speed Aspects of 3-D Aircraft Intakes, Modelling With & Without Ground Effect, In Presence of Cross-wind & Lip-flow Separation Prediction", CEAS 7th European Propulsion Forum "Aspects of Engine / Airframe Integration", March 1999, Pau, France.

[8] GUPTA, K.K., "STARS - An Integrated Multi-disciplinary Solver", NASA TM 4795, 1997.

[9] NANGIA, R.K. & PALMER, M.E., "Negatively Scarfed Inlets for Acoustic Reduction, Aerodynamic Performance Assessment", 38th Aerospace Sciences Meeting & Exhibit, AIAA 2000-0354, January 2000, Reno, NV.

[10] NANGIA, R.K. & PALMER, M.E., "Inlets with Negative Scarf for Acoustic Reduction, Aerodynamic Performance Assessment at Transonic Speeds", 18th Applied Aerodynamics Meeting, AIAA 2000-4409, August 2000, Colorado, USA.

[11] NANGIA, R.K., "An Inverse Design Method for 3 D Intakes", Paper to be published.

## NOMENCLATURE

| | |
|---|---|
| $A_0$ | Capture Area |
| $A_c$ | Highlight Area |
| $A_t$ | Throat Area |
| CR | =Ac/At, Contraction Ratio |
| $D_h$ | or d, Diameter of the Highlight Area |
| LE | Leading Edge |
| $M_0$ | Free-stream Mach Number |
| M | Mach Number |
| $M_{EF}$ | Mach Number at Engine Face |
| $M_T$ | Mach Number at throat |
| MFR | Mass Flow Ratio, A0/Ac |
| Re | Reynolds number based on Dh |
| V | Velocity, Freestream, Usually taken as unity |

$V_{EF}$ Velocity at Engine Face

$\alpha$ Angle of Attack, measured at Inlet axis

$\beta$ Angle of Side-slip

L Highlight Plane Scarf angle

$\Phi$ Displacement Angle about Inlet Highlight (Bottom = 0°)

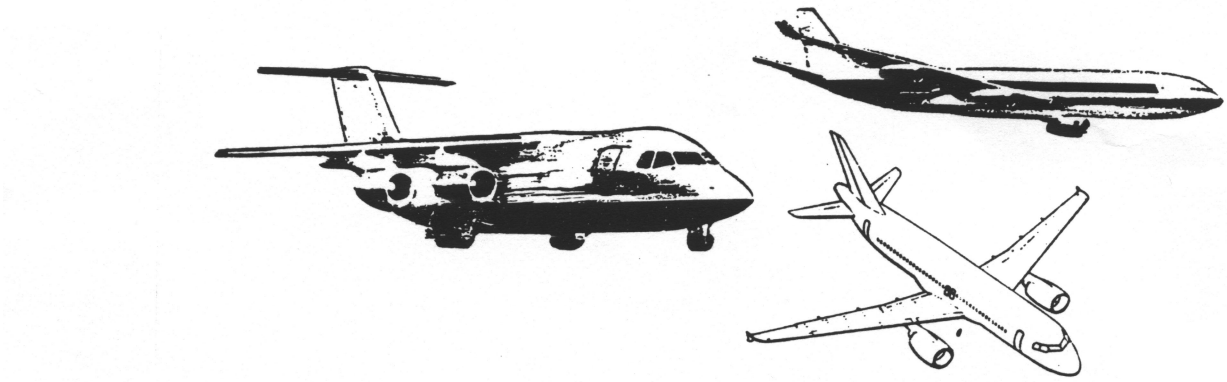

FIG. 1 TRANSPORT AIRCRAFT ENGINE INLET INSTALLATIONS

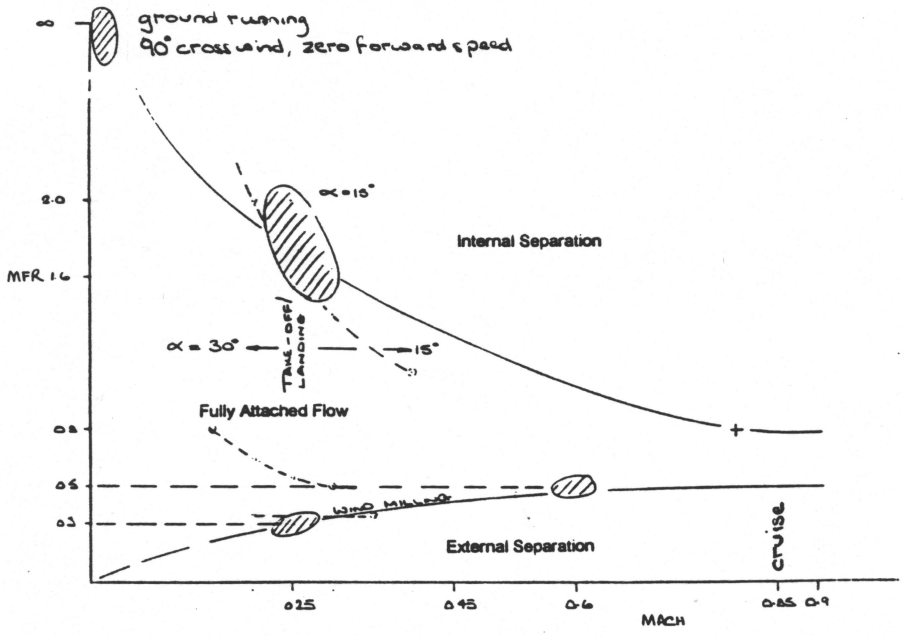


FIG. 2 TYPICAL TRANSPORT ENGINE OPERATING ENVELOPE

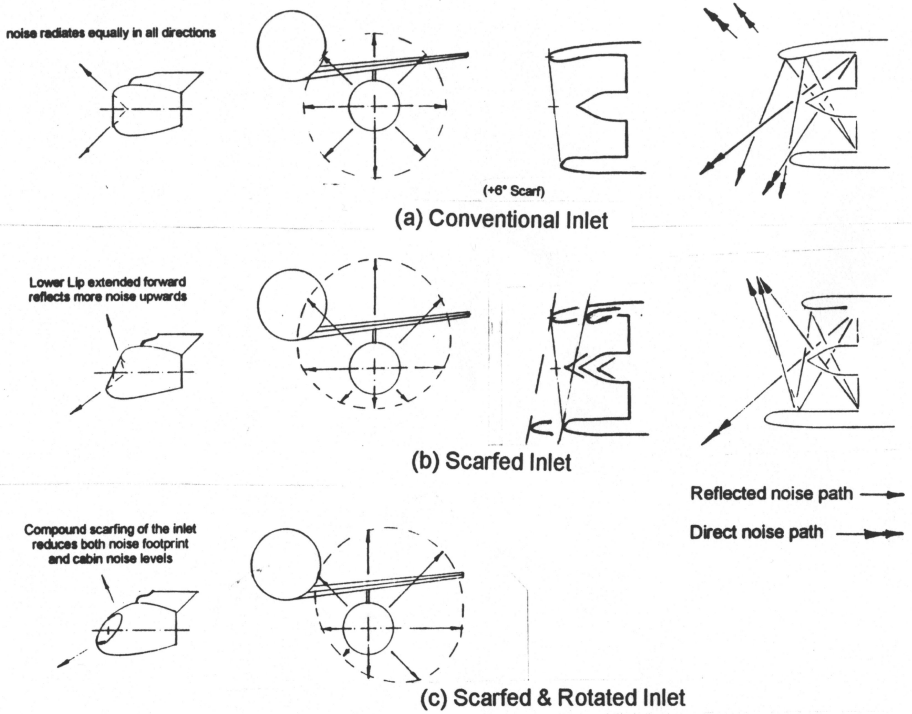


FIG. 3 INLET NOISE GENERATION, REDUCING NOISE FOOTPRINT

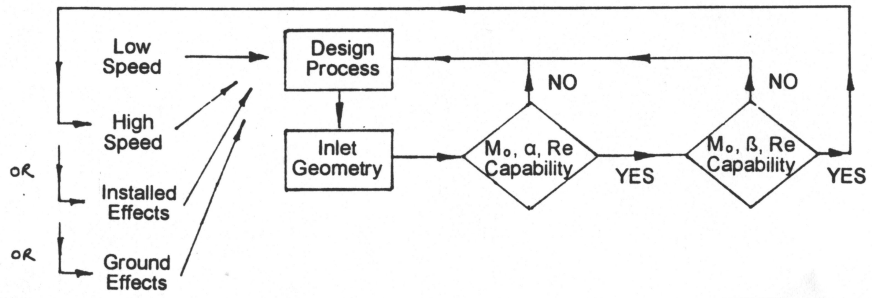


FIG. 4 POSSIBLE ITERATIVE INLET DESIGN PROCESS

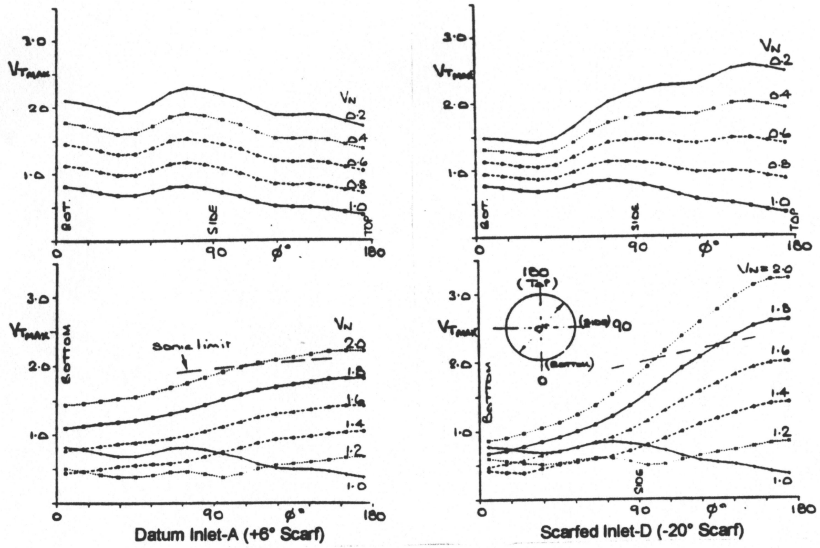


FIG. 5 $V_{T\,max}$ VARIATION WITH $V_N$ AROUND INLET, $M_0 = 0.25$, $\alpha = 0°$

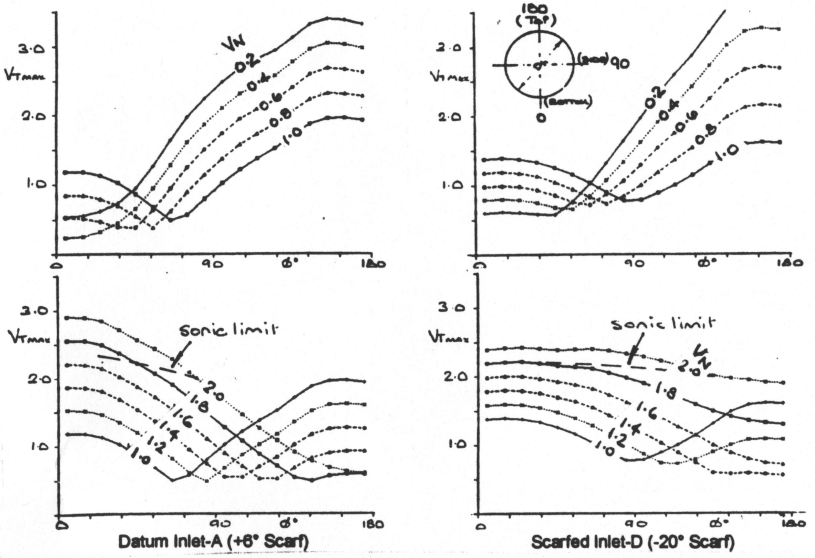


FIG. 6 $V_{T\,max}$ VARIATION WITH $V_N$ AROUND INLET, $M_0 = 0.25$, $\alpha = 20°$

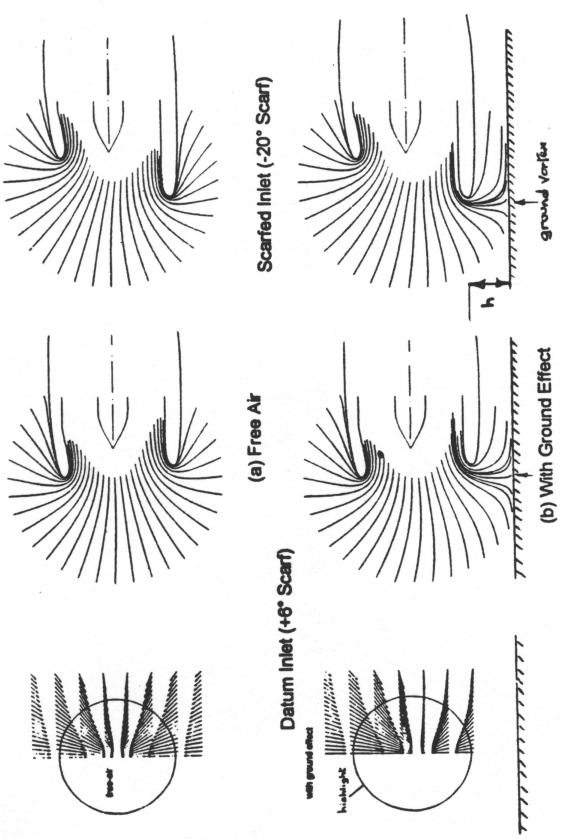


FIG. 10 FLOW VECTORS, STREAMLINES & $V_{T\,max}/V_N$ VARIATION, SCARFED INLETS, ZERO-SPEED, WITH & WITHOUT GROUND EFFECT

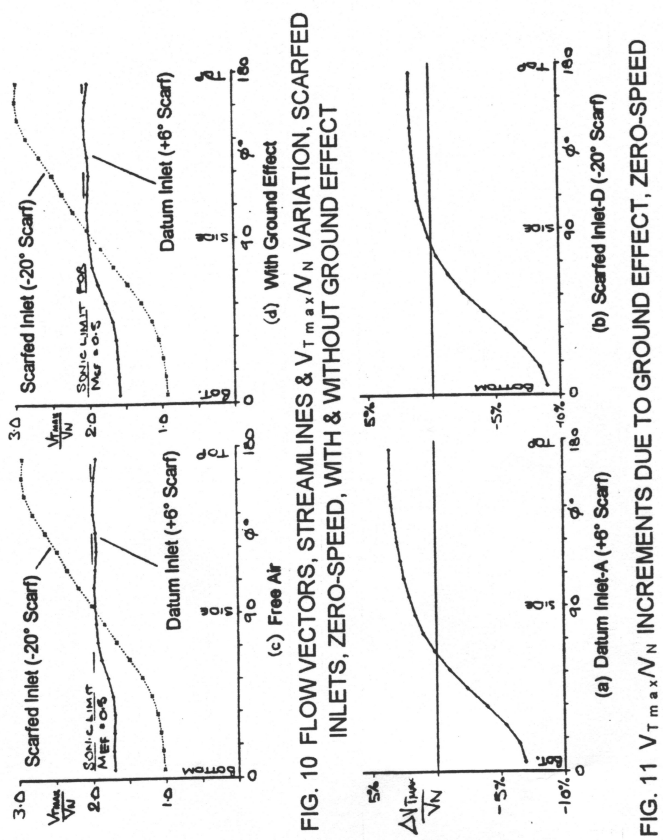





FIG. 11 $V_{T\,max}/V_N$ INCREMENTS DUE TO GROUND EFFECT, ZERO-SPEED

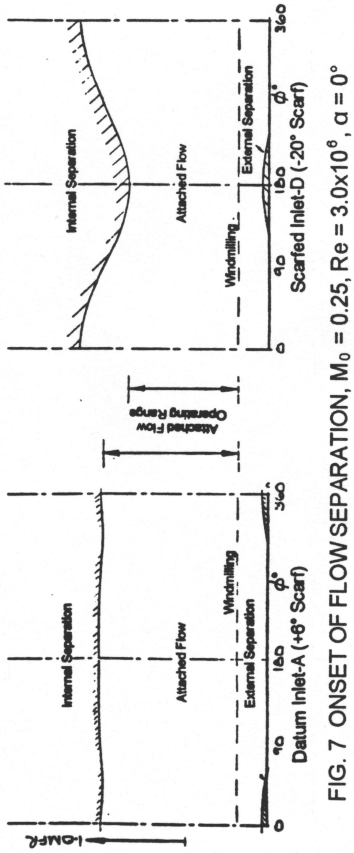


FIG. 7 ONSET OF FLOW SEPARATION, $M_0 = 0.25$, $Re = 3.0 \times 10^6$, $\alpha = 0°$

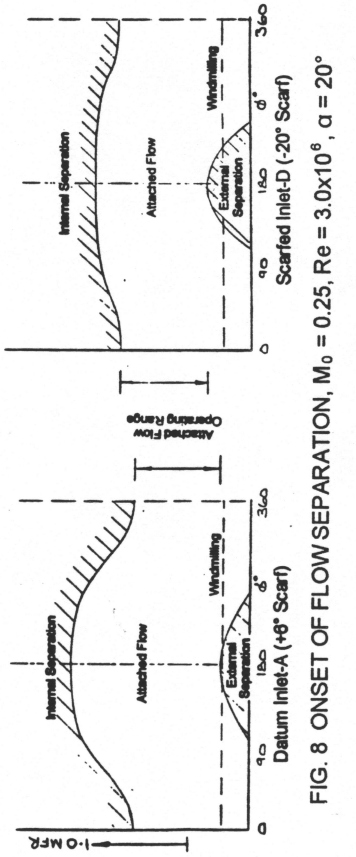


FIG. 8 ONSET OF FLOW SEPARATION, $M_0 = 0.25$, $Re = 3.0 \times 10^6$, $\alpha = 20°$

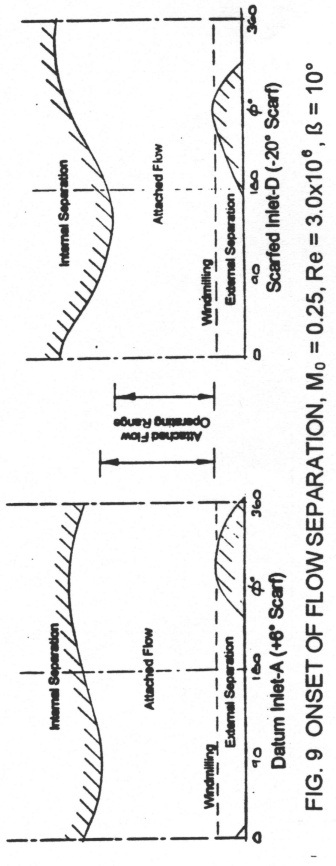


FIG. 9 ONSET OF FLOW SEPARATION, $M_0 = 0.25$, $Re = 3.0 \times 10^6$, $\beta = 10°$

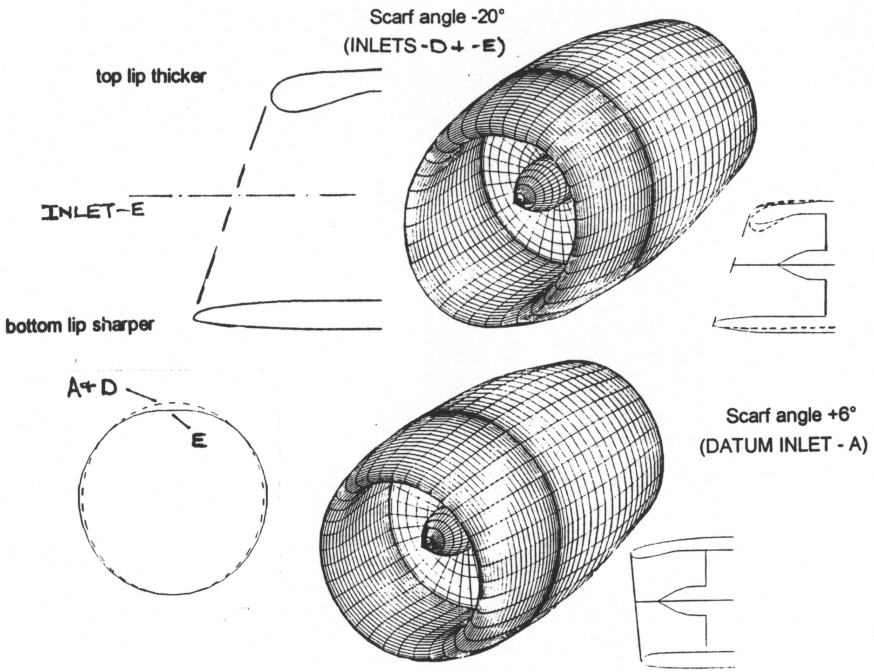


FIG. 12 -20° SCARF (DESIGNED) INLET PROFILE

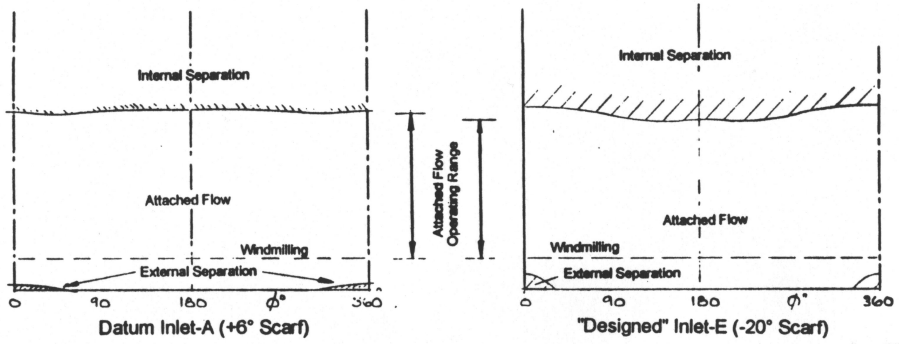


FIG. 13 ONSET OF FLOW SEPARATION, $M_0 = 0.25$, $Re = 3.0 \times 10^6$, $\alpha = 0°$

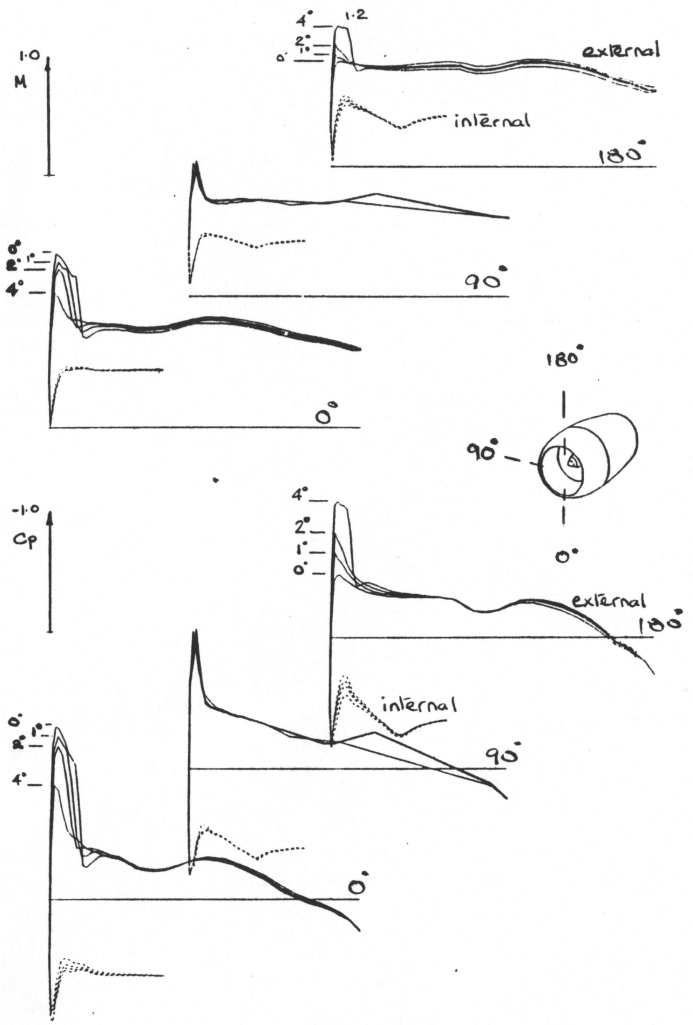


FIG. 14 DATUM INLET-A, MACH NO. & Cp DISTRBNS, STNS $\Phi = 0°$, 90° & 180°, $M_0 = 0.8$, $M_{EF} = 0.5$, $\alpha = 0°$, 1°, 2° & 4°

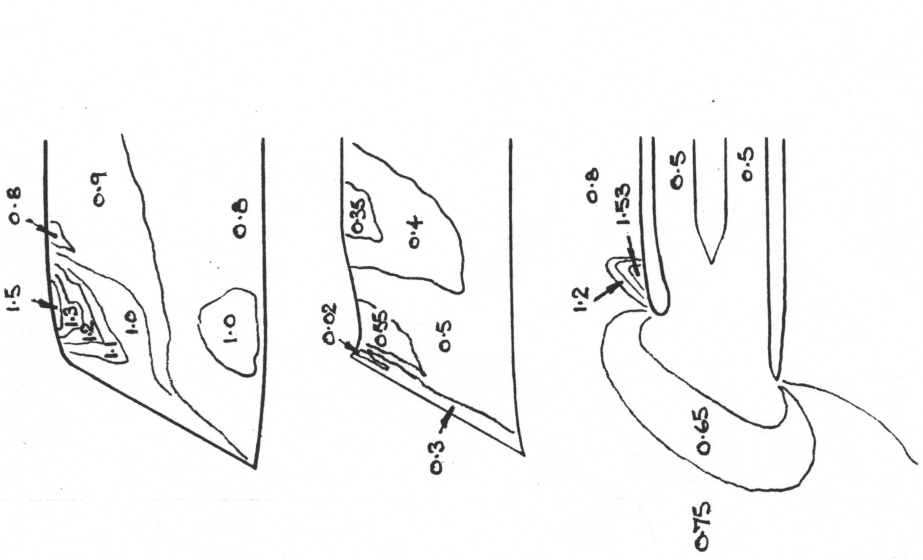

FIG. 17 "DESIGNED" INLET-E, $M_0 = 0.8$, $M_{EF} = 0.5$, $\alpha = 0°$, MACH No. CONTOURS ON OUTER & INNER SURFACES & MEAN PLANE

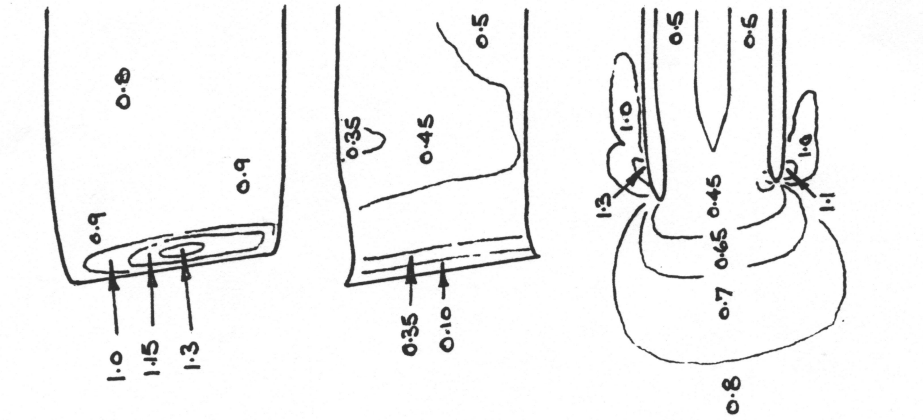

FIG. 16 DATUM INLET-A, $M_0 = 0.8$, $M_{EF} = 0.5$, $\alpha = 4°$, MACH No. CONTOURS ON OUTER & INNER SURFACES & MEAN PLANE

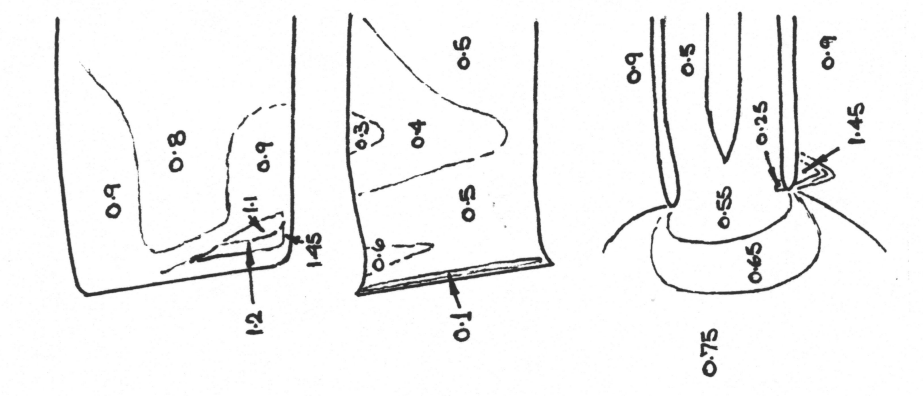

FIG. 15 DATUM INLET-A, $M_0 = 0.8$, $M_{EF} = 0.5$, $\alpha = 0°$, MACH No. CONTOURS ON OUTER & INNER SURFACES & MEAN PLANE

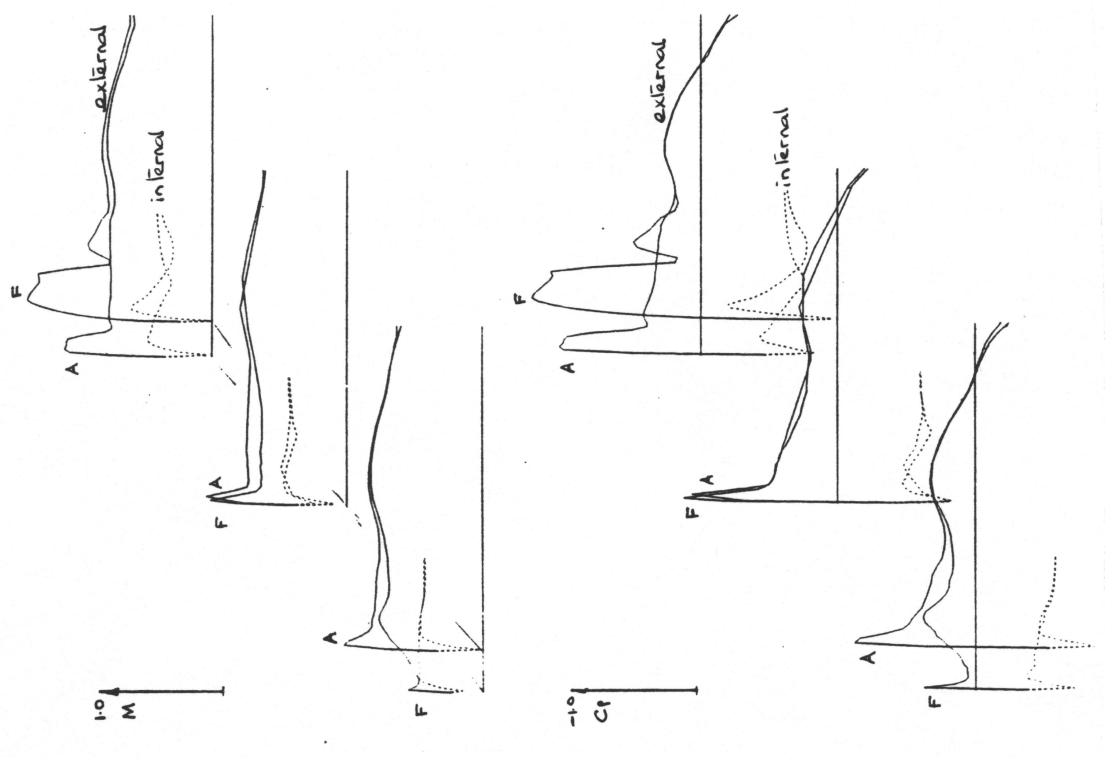


FIG. 19 DATUM INLET-A & "DESIGNED" INLET-F, MACH NO. & Cp DISTRBNS, STNS Φ = 0°, 90° & 180°, $M_0$ = 0.8, $M_{EF}$ = 0.5, α = 4°

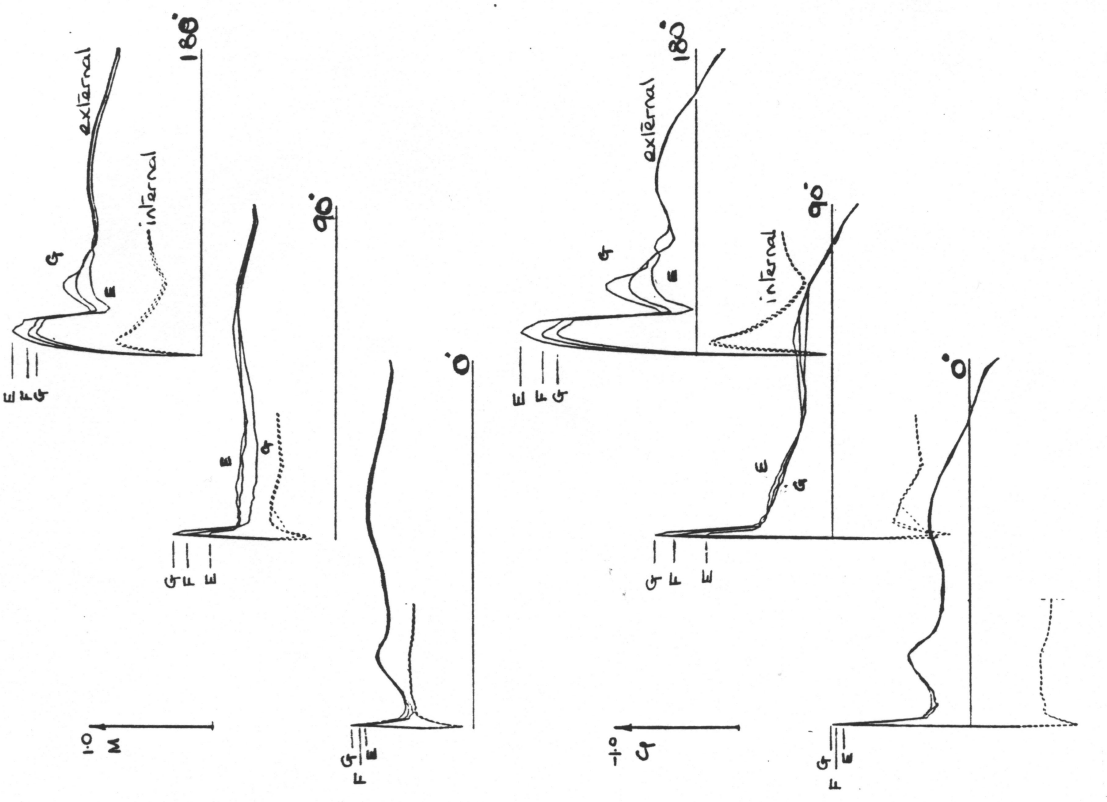


FIG. 18 "DESIGNED" INLETS-E, -F & -G, EFFECT OF CAMBER, MACH NO. & Cp DISTRBNS, STNS Φ = 0°, 90° & 180°, $M_0$ = 0.8, $M_{EF}$ = 0.5, α = 0°